university of groningen

Low-Frequency Variability in a Low-Order Shallow Water Atmospheric Model

Alef Sterk
University of Groningen
a.e.sterk@rug.nl

Renato Vitolo
University of Exeter
r.vitolo@ex.ac.uk

Henk Broer
University of Groningen
h.w.broer@rug.nl

Carles Simó
Universitat de Barcelona
carles@maia.ub.es

Henk Dijkstra
Utrecht University
h.a.dijkstra@uu.nl

Abstract

Low-frequency variability is investigated in a low-order atmospheric model derived from the 2-layer shallow water equations on a β-plane channel with bottom topography.

- Low-frequency variability in our model:
  - variability on time scales from 10 to 200 days on a zonal wavenumber 3 (Benzi & Speranza 1989);
  - irregular weakening and amplification of non-propagating planetary waves;
  - related to strange attractors through bifurcations of periodic orbits;
  - dominant time scales and spatial patterns: inherited from periodic orbits;
  - persistent in parameter space.
- New scenario: available theories (Charney & DeVore 1979, Legras & Ghil 1985, Crommelin et al. 2004) rely on multiple equilibria and unrealistic zonal windspeeds.

Model

- 46-dimensional; obtained from SW equations by Galerkin projection on wavenumbers 0,3 (zonal) and 0,1,2 (meridional).
- Forced by zonal wind profile with magnitude U_0.
- Planetary-scale channel (29000×2500 km).
- Pressure in each layer

$$p_1 = \rho_1 g(h_1 + h_2 + h_b - z)$$
$$p_2 = \rho_1 g h_1 + \rho_2 g(h_2 + h_b - z)$$

- Dynamical equation in each layer

$$u_t + uu_x + vu_y = -\frac{p_x}{\rho} + (f + \beta y)v - \mu(u - u^*) + A\Delta u - ru$$
$$v_t + uv_x + vv_y = -\frac{p_y}{\rho} - (f + \beta y)u - \mu(v - v^*) + A\Delta v - rv$$
$$h_t + uh_x + vh_y = -h(u_x + v_y)$$

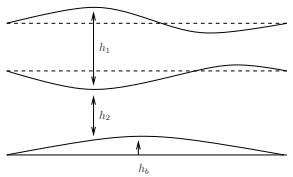

Figure 1: *Setup of the 2-layer shallow water model. Each layer has a constant density and variable thickness.*

Bifurcations

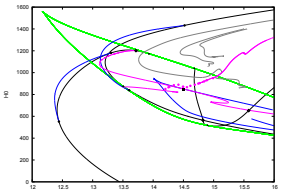

Figure 2: *Bifurcation curves in the (U_0, h_0)-plane: saddle-node bifurcation of equilibria (green), Hopf bifurcation of equilibria (black), saddle-node bifurcation of periodic orbits (blue), period doubling bifurcations (grey), and Neimark-Sacker bifurcations (magenta).*

- Bifurcations of equilibria and periodic orbits:
  - control parameters: magnitude of zonal wind forcing (U_0) and topographic height (h_0);
  - there exist two different branches of periodic orbits: $h_0 \leq 950$: period 10 days, traveling wave; $h_0 \geq 950$: period 50 days, non-propagating wave
  - codimension-2 points: Hopf-saddle-node of equilibria (triangles) and periodic orbits (square), generalized Hopf (circle), double Hopf (diamond);
- Routes to chaos:
  - period-doubling cascade;
  - breakdown of a 2-torus attractor after a Neimark-Sacker bifurcation;
  - saddle-node bifurcations of periodic orbits.

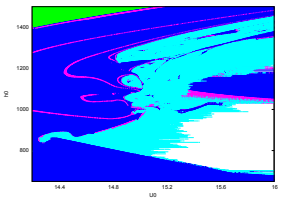

Figure 3: *Lyapunov diagram of attractors. Equilibria (green), periodic attractors (blue), 2-torus attractors (magenta), and strange attractors (cyan).*

- Occurrence of attractors:
  - strange attractors appear when $14 \leq U_0 \leq 16$ and $650 \leq h_0 \leq 1500$;
  - islands of periodic behaviour in the middle of chaos.

Strange attractor I

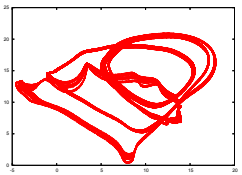

Figure 4: *Strange attractor after period doubling cascade ($U_0 = 15, h_0 = 1200$).*

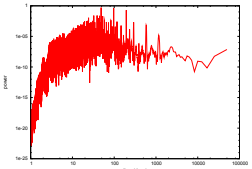

Figure 5: *Power spectrum: dominant time scale approximately 50 days; peaks at multiples of 50 days due to period doublings.*

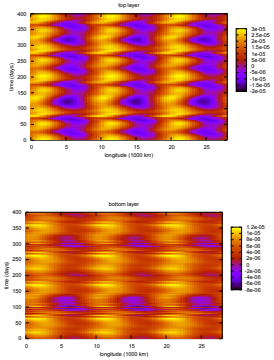

Figure 6: *Hovmöller diagram of vorticity along a line of constant latitude: irregular weakening and amplification of vorticity field; non-propagating character; variability stronger in upper layer.*

Strange attractor II

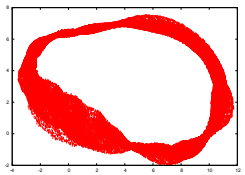

Figure 7: *Strange attractor after breakdown of a 2-torus attractor ($U_0 = 14.78, h_0 = 900$).*

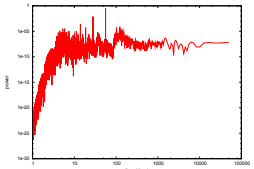

Figure 8: *Power spectrum: dominant time scales are 20 and 60 days; two peaks are inherited from the formerly existing 2-torus.*

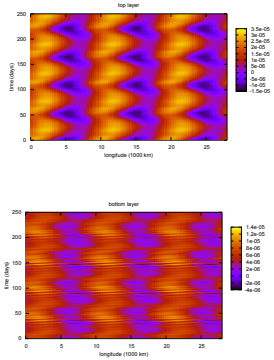

Figure 9: *Hovmöller diagram of vorticity along a line of constant latitude: irregular weakening and amplification of vorticity field; non-propagating character; time scales different for both layers.*

Conclusions

- Summary of dynamical scenario:
  - Hopf bifurcations give rise to two different branches of periodic orbits;
  - periodic attractors bifurcate into strange attractors via three different routes to chaos;
  - strange attractors are related to irregular weakening and amplification of vorticity field;
- The dynamical mechanisms in our model are very different from the available theories (Legras & Ghil 1985, Crommelin et al. 2004).
- Future work:
  - focus on the dynamics around the codimension-2 points in the parameter plane;
  - determination of the boundaries of the periodic islands within the chaotic zone;
  - investigate whether the current dynamical scenarios persist when the number of retained modes in the Galerkin projection is increased.

References

[1] R. Benzi and A. Speranza: *J. Climate*, **2** (1989), 367 – 379.

[2] H.W. Broer, C. Simó, and R. Vitolo: *Nonlinearity* **15(4)** (2002), 1205 – 1267.

[3] J.G. Charney and J.G. DeVore: *J. Atmos. Sci.*, **36** (1979), 1205 – 1216.

[4] D.T. Crommelin, J.D. Opsteegh, and F. Verhulst: *J. Atmos. Sci.* **61(12)** (2004), 1406 – 1419.

[5] H. Itoh and M. Kimoto: *J. Atmos. Sci.* **53** (1996), 2217 – 2231.

[6] B. Legras and M. Ghil: *J. Atm. Sci.* **42** (1985), 433 – 471.

[7] P. Malguzzi, A. Speranza, A. Sutera, and R. Caballero: *J. Atmos. Sci.*, **54** (1997), 2441 – 2451.

[8] L. van Veen: *Int. J. Bifur. Chaos* **13** (2003), 2117 – 2139.

European Geosciences Union General Assembly 2009, April 19 – 24, Vienna, Austria